Proceedings of Meetings on Acoustics

Volume 29 http://acousticalsociety.org/

172nd Meeting of the Acoustical Society of America

Honolulu, Hawaii
28 November - 2 December 2016

Engineering Acoustics: Paper 4pEA2

Virtual Sensing Technique for Feedforward Active Noise Control

Shoma Edamoto
Faculty of Engineering Science, Kansai University, Japan; k125664@kansai-u.ac.jp

Chuang Shi
School of Electrical and Electronic Engineering, Nanyang Technological University, Singapore; shichuang@ntu.edu.sg

Yoshinobu Kajikawa
Faculty of Engineering Science, Kansai University, Japan; kaji@kansai-u.ac.jp

Active noise control (ANC) is a promising technique to reduce unwanted acoustic noise, based on the superposition property of acoustic waves. When an anti-noise wave is elegantly generated to have the same amplitude and inverse phase of the noise wave, ANC can reduce the noise level at the desired location, where an error microphone is placed to monitor the error signal and make the whole system a closed-loop control problem. In the case when the error microphone cannot be placed at the desired noise reduction location, virtual sensing techniques are useful. In this paper, we examine a recently proposed virtual sensing technique in an experimental setup using the parametric array loudspeaker as the anti-noise source (also known as the secondary source). Experiment results show that improved noise reduction can be achieved at the virtual microphone location.

Published by the Acoustical Society of America

 [DOI: 10.1121/2.0000478]

1. INTRODUCTION

In general, ANC systems are categorized into feedback control systems that deal with predicable narrowband noise and feedforward control systems that utilize time-advanced information to reduce broadband noise [1]–[3]. The optimum noise reduction performance is achieved at the error microphone location. When the error microphone is unable to be placed at the desired location, virtual sensing techniques are necessary to be carried out [4]–[8].

In this paper, we work on an experimental setup of the feedforward ANC system that uses a parametric array loudspeaker as the secondary source. The parametric array loudspeaker is also known as the ultrasonic loudspeaker that transmits a modulated ultrasonic wave to create an audio beam by the nonlinearity of air [9], [10]. Using such a directional loudspeaker as the secondary source in an ANC system has the advantage of minimizing the spillover effect [11]–[14]. A dummy head is adopted to examine the noise reduction at the eardrum, which is also the targeted virtual microphone location. The virtual sensing technique, previously proposed by the authors [7], is examined in situations when the error microphone location is not ideal and the primary path is changing.

2. Feedforward ANC system with the virtual sensing technique

A. Zone of quietness in the ANC system

The zone of quietness (ZoQ) is achieved in the vicinity of the error microphone in an ANC system. While the noise control filter is being updated, the output of the error microphone is iteratively minimized in the least mean square sense. The size of the ZoQ is known to be approximated by 1/10 of the wavelength of the noise wave around the error microphone in the single-channel ANC system and relatively larger in the multi-channel ANC system [2], [15]. However, in some practical cases, the error microphone has to be placed far away from the desired location. Hence, minimizing the output of the error microphone cannot guarantee an adequate noise reduction at the desired location. Consumer ANC systems, such as the noise canceling headphone, head-mounted ANC system, and ANC headrest, aim to reduce the noise level at the eardrum of the listener. When the wavelength of the noise wave is of a sufficient length, placing the error microphone at the entrance of the ear canal is an acceptable solution. However, when the noise contains noticeable power in the frequency range above 500 Hz, it is necessary to work out an ANC system with the virtual sensing technique that can realize the noise reduction at the desired location without placing the error microphone there.

B. The virtual sensing technique using an auxiliary filter

Figure 1 shows the block diagram of the feedforward ANC system with our proposed virtual sensing technique, where $P(z)$ is the transfer function of the primary path from the reference microphone to the error microphone; $V(z)$ is the transfer function of the virtual primary path from the reference microphone to the virtual microphone; $S(z)$ is the transfer function of the secondary path from the secondary source to the error microphone; and $S_v(z)$ is the transfer function of the virtual secondary path from the secondary source to the virtual microphone. This ANC system achieves the optimum noise reduction at the virtual microphone location through two stages of implementation.

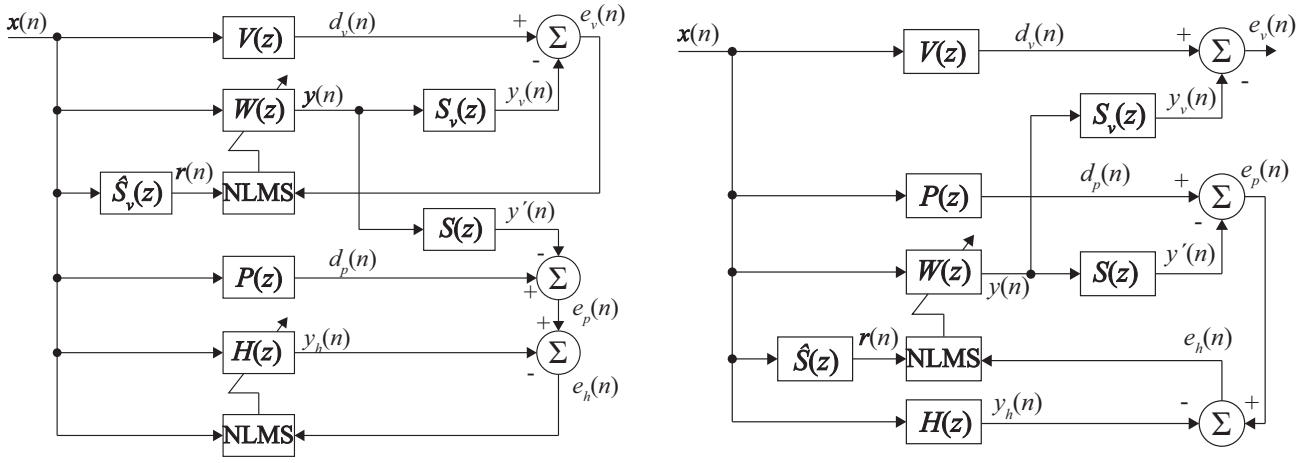

(a) Tuning stage

(b) Control stage

Figure 1: Block diagram of the feedforward ANC system with the virtual sensing technique (extracted from [7]).

In the tuning stage, the output of the noise control filter is expressed as

$$Y(z) = W(z)X(z), \tag{1}$$

where $W(z)$ is the noise control filter and $X(z)$ is the reference signal. An auxiliary filter $H(z)$ is introduced, of which the output is expressed as

$$Y_h(z) = H(z)X(z). \tag{2}$$

The coefficients of the noise control filter and the auxiliary filter are updated by

$$\mathbf{w}(n+1) = \mathbf{w}(n) + \frac{\alpha_c}{\beta_c + \|\mathbf{r}(n)\|^2}\mathbf{r}(n)e_v(n) \tag{3}$$

and

$$\mathbf{h}(n+1) = \mathbf{h}(n) + \frac{\alpha_h}{\beta_h + \|\mathbf{x}(n)\|^2}\mathbf{x}(n)e_h(n), \tag{4}$$

where the filtered reference signal for the FXNLMS algorithm is calculated as

$$\mathbf{r}(n) = \hat{\mathbf{s}}_v^T\mathbf{x}(n); \tag{5}$$

α_c and α_h are the step size parameters; β_c and β_h are the regularization parameters for the noise control filter and the auxiliary filter, respectively.

The error signal at the virtual microphone location in the tuning stage is written as

$$\begin{aligned} E_v(z) &= D_v(z) - Y_v(z) \\ &= [V(z) - S_v(z)W(z)]X(z). \end{aligned} \tag{6}$$

Hence, the power of the error signal is expressed as

$$E_v^2(z) = [V^2(z) - 2V(z)S_v(z)W(z) + S_v^2(z)W^2(z)]X^2(z). \tag{7}$$

The gradient of (7) with respect to $W(z)$ yields

$$\frac{\partial E_v^2(z)}{\partial W(z)} = 2[S_v(z)W(z) - V(z)]S_v(z)X^2(z). \tag{8}$$

Therefore, the optimum noise control filter converges to

$$W^o(z) = \frac{V(z)}{S_v(z)}. \tag{9}$$

At the same time, the error signal used to update the auxiliary filter $H(z)$ contains the error signal at the virtual microphone location and is expressed as

$$\begin{aligned} E_h(z) &= E_p(z) - Y_h(z) \\ &= D_p(z) - Y'(z) - H(z)X(z) \\ &= P(z)X(z) - S(z)W(z)X(z) - H(z)X(z). \end{aligned} \tag{10}$$

Under the assumption that the time scale of convergence is much shorter than that of the environmental change, substituting $W^o(z)$ into (10), we obtain the quasi steady state equation as

$$E_h(z) = P(z)X(z) - \frac{S(z)V(z)X(z)}{S_v(z)} - H(z)X(z). \tag{11}$$

The gradient of the error power with respect to $H(z)$ are expressed as

$$\frac{\partial E_h^2(z)}{\partial H(z)} = 2\left[H(z) - P(z) + \frac{S(z)V(z)}{S_v(z)}\right]X^2(z). \tag{12}$$

Therefore, the optimum auxiliary filter converges to

$$H^o(z) = P(z) - \frac{S(z)V(z)}{S_v(z)} = P(z) - S(z)W^o(z). \tag{13}$$

It can be seen from $H^o(z)$ that the auxiliary filter contains the information of the optimum noise control filter at the virtual microphone location.

In the control stage, the error signal at the virtual microphone location is not available to update the noise control filter because there is no physical microphone. The updating algorithm of the noise control filter is thus modified based on Fig. 1(b) as

$$\mathbf{w}(n+1) = \mathbf{w}(n) + \frac{\alpha_c}{\beta_c + \|\mathbf{r}(n)\|^2}\mathbf{r}(n)e_h(n), \tag{14}$$

where the estimate of the error signal at the virtual microphone location is calculated as

$$e_h(n) = e_p(n) - \sum_{i=0}^{K-1} h(i)x(n-i); \tag{15}$$

K is the tap length of the auxiliary filter; and $\mathbf{r}(n)$ is still the filtered reference signal. The z domain expression of (15) is written as

$$\begin{aligned} E_h(z) =& E_p(z) - H(z)X(z) \\ =& [P(z)X(z) - S(z)W(z)X(z)] - \left[P(z) - \frac{S(z)V(z)}{S_v(z)}\right]X(z) \\ =& \left[\frac{V(z)}{S_v(z)} - W(z)\right]S(z)X(z). \end{aligned} \tag{16}$$

Therefore, the optimum noise reduction is preserved at the virtual microphone location.

When the primary path and the virtual primary path are respectively changed by $\Delta P(z)$ and $\Delta V(z)$, the error signal used for updating the noise control filter $W(z)$ is expressed as

$$\begin{aligned} E_h(z) =& E_p(z) - H(z)X(z) \\ =& \{[P(z) + \Delta P(z)]X(z) - S(z)W(z)X(z)\} - \left[P(z) - \frac{S(z)V(z)}{S_v(z)}\right] X(z) \\ =& \left[\frac{\Delta P(z)}{S(z)} + \frac{V(z)}{S_v(z)} - W(z)\right] S(z)X(z). \end{aligned} \tag{17}$$

Therefore, the noise control filter converges to

$$W_a(z) = \frac{\Delta P(z)}{S(z)} + \frac{V(z)}{S_v(z)}. \tag{18}$$

However, the optimum noise control filter should be expressed as

$$W_a^o(z) = \frac{V(z) + \Delta V(z)}{S_v(z)} = \frac{V(z)}{S_v(z)} + \frac{\Delta V(z)}{S_v(z)}. \tag{19}$$

Therefore, the condition to make sure the auxiliary filter $H(z)$ to remain effective is written as

$$\frac{\Delta V(z)}{S_v(z)} = \frac{\Delta P(z)}{S(z)}. \tag{20}$$

Table 1: Experiment parameters.

Tap length of noise control filter W	400
Tap length of auxiliary filter H	400
Tap length of secondary path model	200
Update algorithm of noise control filter W	NLMS
Update algorithm of auxiliary filter H	NLMS
Step size parameter α_c and α_h	0.01
Regularization parameter β_c and β_h	1.0×10^{-6}
Sampling frequency	12000 Hz
Cut-off frequency of analog low-pass filter	2500 Hz

3. Noise reduction experiment

In this section, we examine the effectiveness of the feedforward ANC system with our proposed virtual sensing technique by moving the error microphone and changing the primary path. The fixed-coefficient implementation using an offline trained control filter is used as a benchmark. The experiment parameters are listed in Table 1. The experiment setup is illustrated in Fig. 2. In Fig. 3, a piece of A4 or A2 paper is inserted at 25 cm in front of the primary noise source so that the primary path can be distorted by a small amount. In Fig. 4, the error microphone is depicted to move to 5 cm and 10 cm behind the ear of the dummy head. The secondary path and virtual

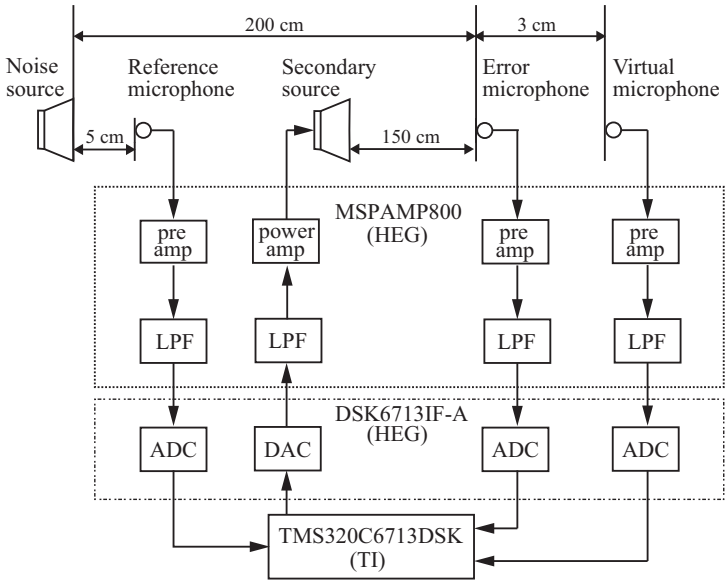

Figure 2: Experiment setup.

Figure 3: A picture showing how the primary path is changed by inserting a piece of paper.

secondary path are offline identified in the tuning stage by a white noise excitation. The primary source plays back another white noise at a sound pressure level of 70 dB calibrated at the virtual microphone location.

Figure 5 shows the spectra of the error signal at the virtual microphone location when the error microphone is placed next to the ear of the dummy head. In Fig. 5 (a), the noise reduction in the band from 500 to 2500 Hz is improved by about 6 dB with the help of the virtual sensing technique. As compared to Fig. 5(b), the ANC system with the virtual sensing technique achieves equivalence

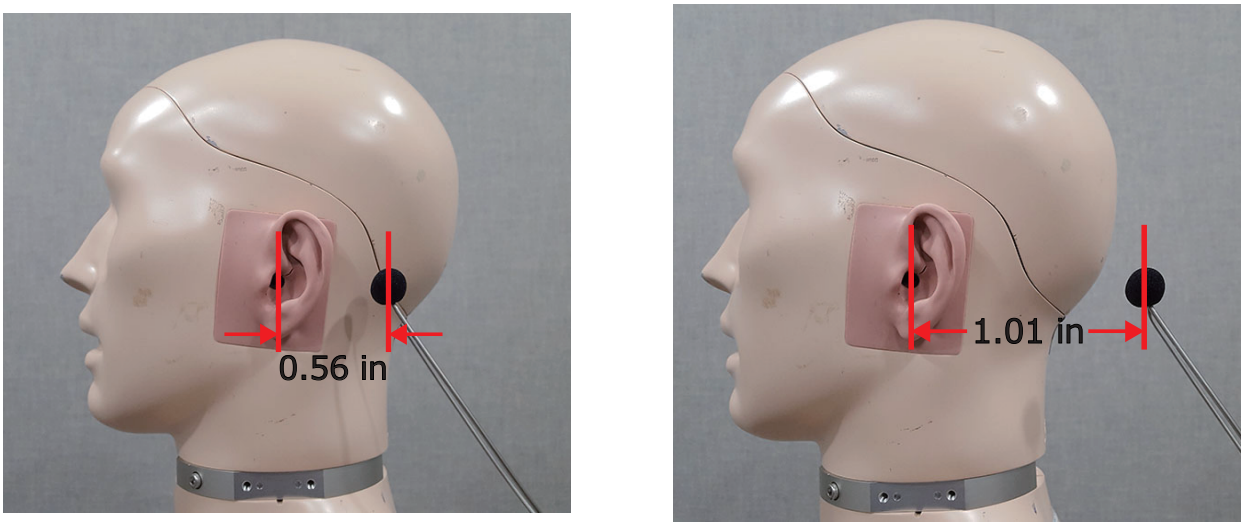

(a) 5 cm (b) 10 cm

Figure 4: The placement of error microphone at (a) 5 cm and (b) 10 cm behind the ear of the dummy head.

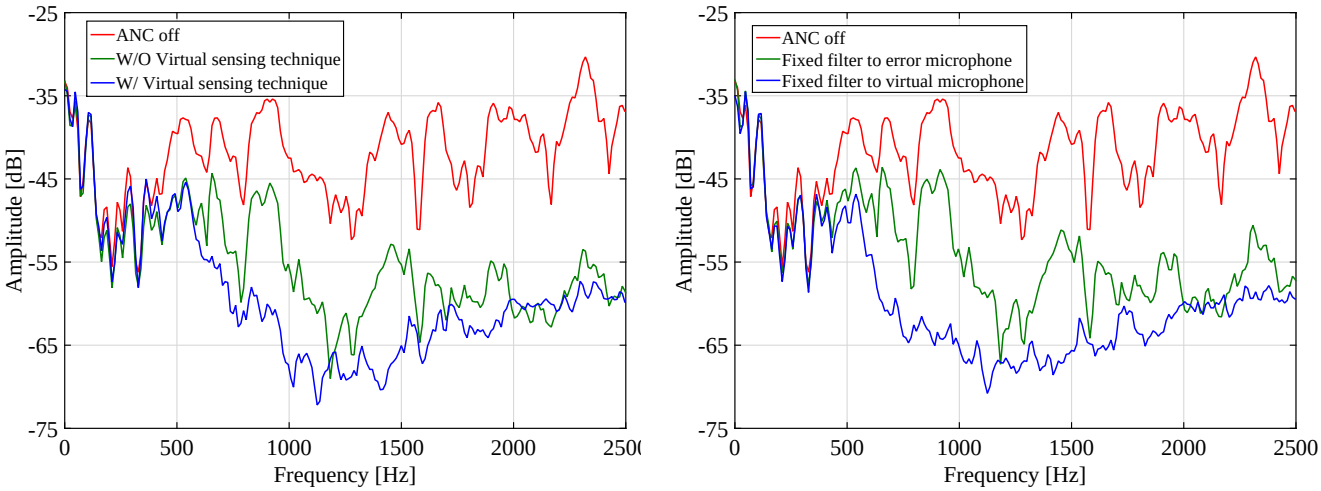

(a) Virtual sensing (b) Fixed filter

Figure 5: Error spectra at the virtual microphone location when error microphone is placed next to the ear of the dummy head.

noise reduction performance to the fixed-coefficient implementation of the optimum noise control filter. Figure 6 shows the spectra of the error signal at the virtual microphone location when the primary path is changed. It is shown in Fig. 6(a) that our proposed virtual sensing technique is able to track the change of the primary path when the error microphone is placed near the opening of the ear canal. In contrast, the fixed coefficient implementation cannot adapt to the change of the primary path as shown in Fig. 6(b).

Figures 7 and 8 demonstrate different cases when both the primary path and secondary path are changed. In Fig. 7, when the error microphone is moved 5 cm behind the ear of the dummy head, the noise reduction performance in the band from 500 to 1250 Hz is easier to maintain as

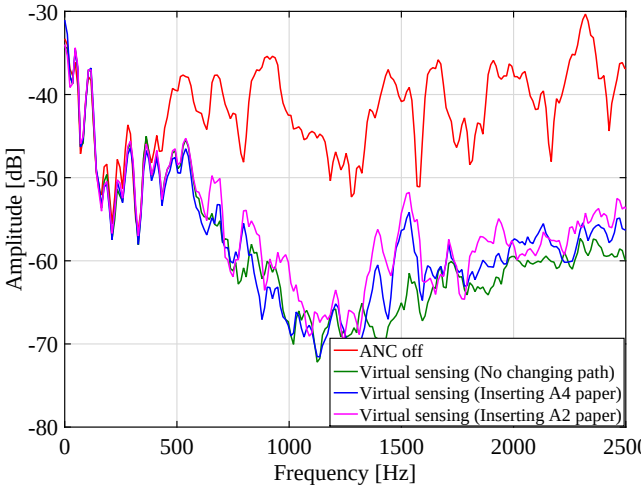

(a) Virtual sensing

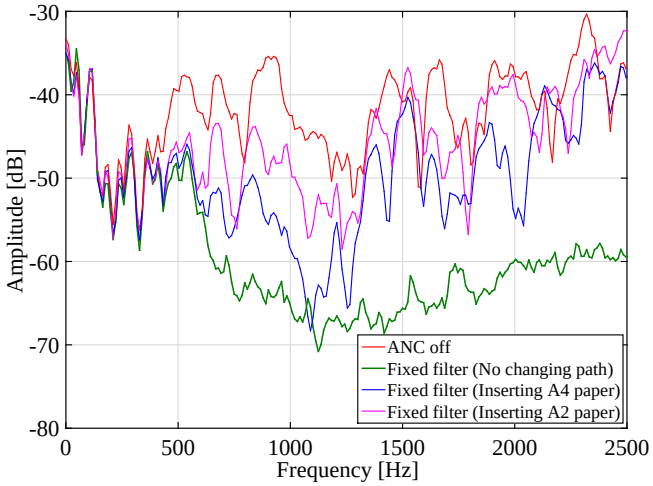

(b) Fixed filter

Figure 6: Error spectra at the virtual microphone location when the primary path is changed by inserting a piece of A2 or A4 paper.

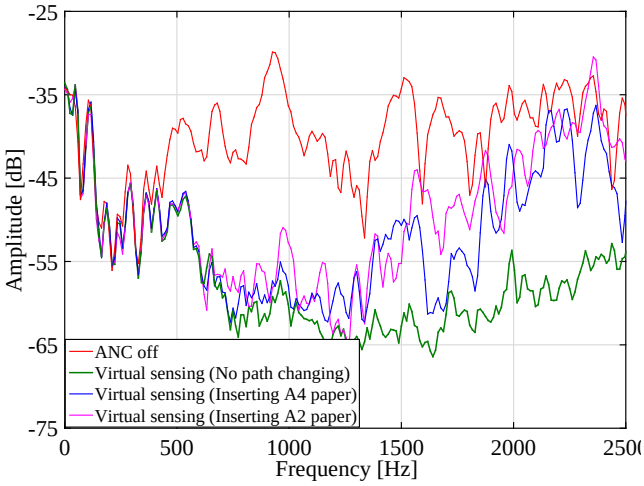

(a) Virtual sensing

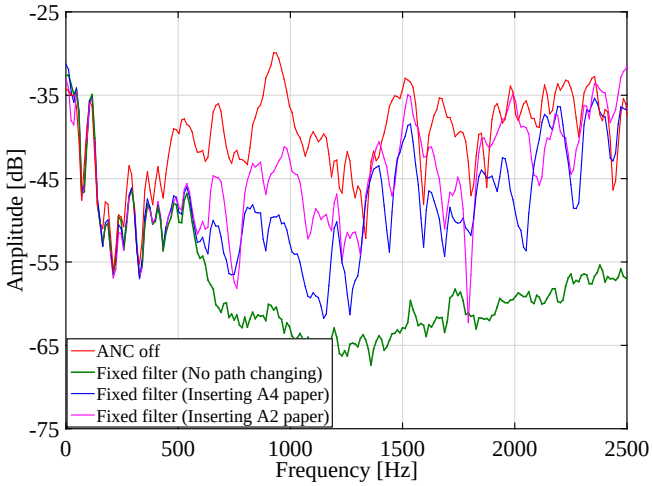

(b) Fixed filter

Figure 7: Error spectra at the virtual microphone location when the error microphone is moved to 5 cm behind the ear of the dummy head and the primary path is changed by inserting a piece of A2 or A4 paper.

compared to the higher frequency band from 1250 to 2500 Hz. This is because inserting a piece of paper affects the higher frequency response more than the lower frequency response. In Fig. 8, as the error microphone is moved further apart from the opening of the ear canal, the noise reduction performance is more degraded. Therefore, in order to cooperate with our proposed virtual sensing technique, placing the error microphone near the opening of the ear canal is necessary.

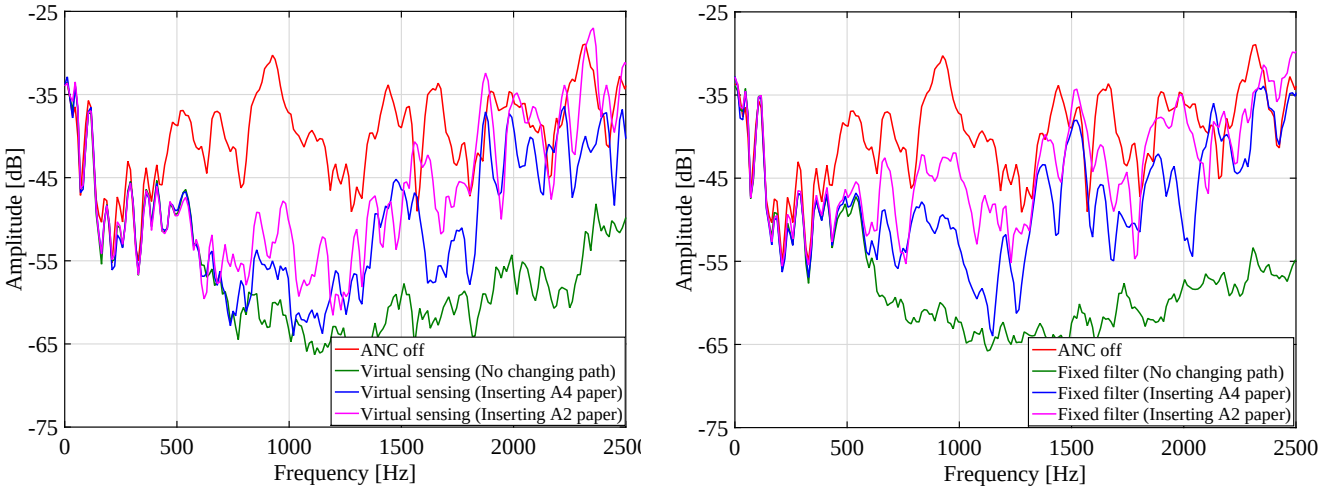

(a) Virtual sensing

(b) Fixed filter

Figure 8: Error spectra at the virtual microphone location when the error microphone is moved to 10 cm behind the ear of the dummy head and the primary path is changed by inserting a piece of A2 or A4 paper.

4. Conclusion

In this paper, the feedforward ANC system with our proposed virtual sensing technique is examined when the primary path and secondary path are not static. The virtual sensing technique is derived based on the introduction of an auxiliary filter. The auxiliary filter can be online identified in the tuning stage. The converged auxiliary filter contains the information of the optimum noise control filter. Therefore, in the control stage, although no physical microphone is placed, the optimum noise reduction is still achieved at the virtual microphone location. The virtual sensing technique is better at maintaining the noise reduction performance of the feedforward ANC system when the error microphone can be placed near the opening of the ear canal. This experimental observation will be analyzed more comprehensively in our future work.

Acknowledgement

This work is supported by MEXT-Supported Program for the Strategic Research Foundation at Private Universities, 2013–2017 and JSPS KAKENHI (15K00256).

References

[1] S. M. Kuo and D. R. Morgan, *Active noise control systems: Algorithms and DSP implementations*. NY: Wiley, 1996.

[2] S. J. Elliott, *Signal processing for active control*. CA: Academic Press, 2001.

[3] Y. Kajikawa, W. S. Gan, and S. M. Kuo, “Recent advances on active noise control: open issues and innovative applications,” *APSIPA Trans. Sign. Inf. Process.*, vol. 1, no. e3, pp. 1–21, Aug. 2012.

[4] M. Pawelczyk, "Adaptive noise control algorithms for active headrest," *Control Eng. Pract.*, vol. 12, no. 9, pp. 1101–1112, Sep. 2004.

[5] M. R. F. Kidner, C. Petersen, A. C. Zander, and C. H. Hansen, "Feasibility study of localised active noise control using an audio spotlight and virtual sensors," in *Proc. Acoust. 2006*, Christchurch, New Zealand, Nov. 2006.

[6] N. Miyazaki and Y. Kajikawa, "Head-mounted active noise control system with virtual sensing technique," *J. Sound Vib.*, vol. 339, pp. 65–83, Mar. 2015.

[7] S. Edamoto, C. Shi, and Y. Kajikawa, "Directional feedforward ANC system with virtual sensing technique," in *Proc. Int. Workshop Smart Info-Media Syst. Asia*, Ayutthaya, Thailand, Sep. 2016.

[8] S. J. Elliott and J. Cheer, "Modeling local active sound control with remote sensors in spatially random pressure fields," *J. Acoust. Soc. Am.*, vol. 137, no. 4, pp. 1936–1946, Apr. 2015.

[9] C. Shi and Y. Kajikawa, "A convolution model for computing the far-field directivity of a parametric loudspeaker array," *J. Acoust. Soc. Am.*, vol. 137, no. 2, pp. 777–784, Feb. 2015.

[10] C. Shi, Y. Kajikawa, and W. S. Gan, "An overview of directivity control methods of the parametric array loudspeaker," *APSIPA Trans. Sign. Inf. Process.*, vol. 3, no. e20, pp. 1–12, Dec. 2014.

[14] L. A. Brooks, A. C. Zander, and C. H. Hansen, "Investigation into the feasibility of using a parametric array control source in an active noise control system," in *Proc. Acoust. 2005*, Busselton, Australia, Nov. 2005.

[12] N. Tanaka and M. Tanaka, "Active noise control using a steerable parametric array loudspeaker," *J. Acoust. Soc. Am.*, vol. 127, no. 6, pp. 3526–3537, Jun. 2010.

[13] K. Tanaka, C. Shi, and Y. Kajikawa, "Binaural active noise control using parametric array loudspeakers," *Applied Acoust.*, vol. 116, pp. 170–176, Jan. 2017.

[14] C. Shi and W. S. Gan, "Using length-limited parametric source in active noise control applications," in *Proc. 20th Int. Congr. Sound Vib.*, Bangkok, Thailand, Jul. 2013.

[15] S. J. Elliott and M. Jones, "An active headrest for personal audio," *J. Acoust. Soc. Am.*, vol. 119, no. 5, pp. 2702–2709, May 2006.